COMPUTATIONAL STUDY OF HEAT TRANSFER IN BUBBLING FLUIDIZED BEDS WITH GELDART A POWDER

Q. F. HOU*, Z. Y. ZHOU and A. B. YU

Laboratory for Simulation and Modelling of Particulate Systems, School of Materials Science and Engineering,

The University of New South Wales, Sydney, NSW 2052, Australia

*Corresponding author, E-mail address: Q.Hou@student.unsw.edu.au

ABSTRACT

Gas fluidization is widely used in industries and has been extensively studied either experimentally or mathematically. Recently, the coupled approach of discrete particle simulation (DPS) for solid phase and computational fluid dynamics (CFD) for gas phase has been proposed to study the heat transfer in fluidized beds at a particle level. The approach offers a convenient way to study the effects of key variables under controlled conditions. In this work, DPS-CFD is used to examine the effects of gas superficial velocity and cohesive force in bubbling fluidized beds with Geldart A powder. It is shown that the convective heat flux increases and the conductive heat flux decreases with the increase of gas superficial velocity. With the increase of cohesive force, the convective heat flux decreases and the conductive heat flux increases. The heat transfer characteristics are analysed in terms of the heat transfer mechanisms such as particle-fluid convection and particle-particle conduction. The related bed structures such as the bed porosity and the average coordination number are obtained and used to explain the heat transfer characteristics.

Keywords: Gas fluidization; Geldart A powder; Discrete particle simulation; Heat transfer

INTRODUCTION

Fluidized beds are widely used in industries for its high performance. To achieve optimal design and control of such a reactor, it is important to understand its underlying flow and heat transfer mechanisms. In the past, many studies have been carried out in this field, and many empirical correlations have been established to determine the heat transfer coefficient (see, for example, reviews by Kunii and Levenspiel, 1991; Molerus and Wirth, 1997). Those studies are mainly macroscopic, focused on the overall heat transfer capability. As a result, the resulting correlations are often of limited applicability. In recent years, heat transfer behaviour in a fluidized bed at a microscopic, individual particle level has been examined experimentally (for example, Collier et al., 2004; Scott et al., 2004). Such particle scale studies are useful but have limitations in exploring the fundamentals. The contribution of different heat transfer mechanisms are difficult to quantify. Moreover, the heat transfer of a particle is strongly affected by the local gas-solid flow structure, and hence varies spatially and temporally. The information derived for a single particle may not be reliable because of the difficulty in quantifying the structural information.

Alternatively, mathematical modelling has been increasingly accepted as an effective method to study the heat transfer phenomenon in particle-fluid systems. The so-called discrete particle simulation (DPS) coupled with computational fluid dynamics (CFD) approach has been attempted by some investigators to investigate different systems (Kaneko et al., 1999; Li and Mason, 2000; Li and Mason, 2002; Zhou et al., 2003; Zhou et al., 2004). But in those studies, the particle-particle conductive heat transfer is only partially considered. This has been improved recently by Zhou et al. (2009). However, the work in the literature mainly focuses on type B powders. Generally, powders used in fluidization can be classified into four types (A, B, C and D) according to their behaviour (Geldart, 1973). Type A powder is characterised by a stable bed expansion stage between minimum fluidization and bubbling velocities because of the presence of particle-particle cohesive force such as van der Waals force. Since the heat transfer is closely related to local gas-solid structures (Cheng et al., 1999), it is expected that powders A and B have different heat transfer mechanisms in gas fluidization.

In this work, the model proposed by Zhou et al. (2009) is extended to investigate the heat transfer characteristics of type A powder in bubbling gas fluidization. The model is described first, and then the effects of gas superficial velocity and inter-particle van der Waals force on the heat transfer behaviour are investigated in terms of heat fluxes of convection and conduction.

MODEL DESCRIPTION

Governing Equations for Solid and Fluid Phases

Governing equations for a particle moving in a fluidized bed with heat exchange can be written as

$$m_i \frac{d\mathbf{v}_i}{dt} = \sum_j (\mathbf{f}_{c,ij} + \mathbf{f}_{d,ij} + \mathbf{f}_{v,ij}) + \mathbf{f}_{pf,i} + m_i \mathbf{g} \qquad (1)$$

$$I_i \frac{d\boldsymbol{\omega}_i}{dt} = \sum_j (\mathbf{T}_{c,ij} + \mathbf{T}_{r,ij}) \qquad (2)$$

$$m_i c_{p,i} \frac{dT_i}{dt} = \sum_{j=1}^{k_i} Q_{i,j} + Q_{i,f} + Q_{i,rad} + Q_{i,wall} \qquad (3)$$

where $\mathbf{v}_i$ and $\mathbf{\omega}_i$ are the translational and rotational velocities. The forces involved are particle-fluid interaction force $\mathbf{f}_{pf,i}$, gravitational force $m_i\mathbf{g}$, and inter-particle forces which include elastic force $\mathbf{f}_{c,ij}$ and viscous damping force $\mathbf{f}_{d,ij}$. The torque acting on particle i includes two components: $\mathbf{T}_{c,ij}$ which is generated by the tangential force and $\mathbf{T}_{r,ij}$, commonly known as the rolling friction torque, which is generated by the asymmetrical normal force. For a particle undergoing multiple interactions, the individual interaction forces and torques are summed for all particles interacting with particle i. The equations to calculate the forces and torques can be found elsewhere (Johnson, 1985; Zhu et al., 2007). k_i is the number of particles exchanging heat with particle i, $Q_{i,j}$ is the heat exchange rate between particles i and j due to conduction, $Q_{i,f}$ is the heat exchange rate between particle i and its local surrounding fluid, $Q_{i,rad}$ is the heat exchange rate between particle i and its surrounding environment by radiation, and $Q_{i,wall}$ is particle-wall heat exchange rate.

The cohesive force $\mathbf{f}_{v,ij}$ considered is van der Waals force. In the present work, this force is given by (Hamaker, 1937; Israelachvili, 1991; Yang et al., 2000)

$$\mathbf{f}_{v,ij} = -\frac{H_a}{6}\frac{64R_i^3R_j^3(h+R_i+R_j)}{(h^2+2R_ih+2R_jh)^2(h^2+2R_ih+2R_jh+4R_iR_j)^2}\cdot\hat{\mathbf{n}}_{ij} \quad (4)$$

where H_a is Hamaker constant, and h is the separation of surfaces along the line of the centres of particles i and j, R_i and R_j are the radii of particles i and j. A minimum separation h_{min} is used to represent the physical repulsive nature and avoid singular attractive force when h equals to zero. This treatment has proved to be valid for particles down to $1\mu m$ (Yang et al., 2000; Dong et al., 2006).

The continuum fluid field is calculated from the continuity and Navier-Stokes equations based on the local average variables. These equations are given in model B formulation. A standard k-ε turbulence model is implemented (Launder and Spalding, 1974). The governing equations of continuity, momentum and heat transfer can be written as

$$\frac{\partial\varepsilon_f}{\partial t}+\nabla\cdot(\varepsilon_f\mathbf{u})=0 \quad (5)$$

$$\frac{\partial(\rho_f\varepsilon_f\mathbf{u})}{\partial t}+\nabla\cdot(\rho_f\varepsilon_f\mathbf{u}\mathbf{u})=-\nabla p-\mathbf{F}_{fp}+\nabla\cdot\tau+\rho_f\varepsilon_f\mathbf{g} \quad (6)$$

$$\frac{\partial(\rho_f\varepsilon_fc_pT)}{\partial t}+\nabla\cdot(\rho_f\varepsilon_f\mathbf{u}c_pT)=\nabla\cdot(c_p\Gamma\nabla T)+(\sum_{i=1}^{k_V}Q_{f,i}+Q_{f,wall})/\Delta V \quad (7)$$

where τ and ε_f are the fluid viscous stress tensor and porosity, respectively, which are given as $\tau=\mu_e[(\nabla\mathbf{u})+(\nabla\mathbf{u})^{-1}]$, $\varepsilon_f=1-\sum V_i/\Delta V$, where V_i is the volume of particle i in the computational cell of volume ΔV. Γ is the fluid thermal diffusivity, defined by μ_e/σ_T.

The pressure gradient force and drag force are considered as main particle-fluid interaction forces. The pressure gradient force can be written as (Crowe et al., 1998)

$$\mathbf{f}_{pgf,i}=-V_{p,i}\nabla P_{d,i} \quad (8)$$

The correlation of Di Felice (1994) is adopted to calculate the drag force, which is given as

$$\mathbf{f}_{d,i}=0.125C_{d0,i}\rho_f\pi d_i^2\varepsilon_i^2|\mathbf{u}_i-\mathbf{v}_i|(\mathbf{u}_i-\mathbf{v}_i)\varepsilon_i^{-\lambda} \quad (9)$$

where $C_{d0,i}=(0.63+4.8/\mathrm{Re}_i^{0.5})^2$, $\mathrm{Re}_i=\rho_f d_{pi}\varepsilon_i|\mathbf{u}_i-\mathbf{v}_i|/\mu_f$, and $\lambda=3.7-0.65\exp[-(1.5-\log_{10}\mathrm{Re}_i)^2/2]$.

By summing all these particle-fluid interaction forces, the volumetric particle-fluid interaction force $\mathbf{F}_{fp}$ in Eq. (6) can be determined by

$$\mathbf{F}_{fp}=\sum_{i=1}^{k_V}(\mathbf{f}_{d,i}+\mathbf{f}_{pgf,i})/\Delta V \quad (10)$$

Generally, there are three heat transfer mechanisms: convection, conduction and radiation. Radiation is of practical importance only at very high temperatures above 800K (Wong and Seville, 2006). It is not significant in the present work due to the low temperature used (200°C). Adiabatic walls are used in the present study and there is no heat exchange between particle/fluid and walls. The equations to determine the heat fluxes due to convection and conduction are described briefly below.

Equations for Convective Heat Flux

The convective HTC and heat flux between particles and fluid are based on the following equations

$$Nu_i=h_{i,conv}d_{pi}/k_f=2.0+a\mathrm{Re}_i^b\mathrm{Pr}^{1/3} \quad (11)$$

$$Q_{i,f}=h_{i,conv}A(T_f-T_i) \quad (12)$$

where k_f and d_{pi} are the fluid thermal conductivity and particle diameter respectively. Re_i is the local relative Reynolds number for particle i. The air Prandtl number, Pr, is assumed to be 0.712, a constant corresponding to that for air at 300K. a and b are two parameters set to 1.2 and 0.5, respectively (Zhou et al., 2009). $Q_{i,f}$ is the convective heat flux from surrounding fluid to particle i. A is the surface area of particle i exposed to fluid. T_i and T_f are the temperatures of particle i and surrounding fluid, respectively.

Equations for Conductive Heat Fluxes
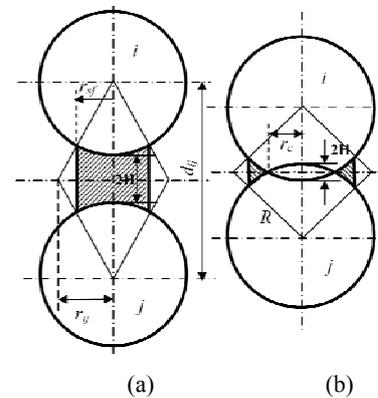
Figure 1: Schematic of the relative position of two spheres: (a) non-contact; and (b) contact with an overlap (Zhou et al., 2009).

Conduction between particles involves various mechanisms, which mainly includes (i) particle-fluid-particle conduction through gas phase including non-contact (Figure 1a) and contact (Figure 1b) conditions; and (ii) particle-particle static and collisional contact conduction (as shown in Figure 1). The equation modified by Zhou et al. (2009) after Cheng et al. (1999) is used in the present work. The particle-fluid-particle conduction is based on the following equation to determine the heat flux between particles i and j

$$Q_{i,j} = (T_j - T_i) \int_{r_{sij}}^{r_{sf}} 2\pi \cdot r((\sqrt{R^2 - r^2} - r(R+H)/r_{ij}) \cdot (1/k_{pi} + 1/k_{pj}) + 2[(R+H) - \sqrt{R^2 - r^2}]/k_f)^{-1} dr \tag{13}$$

The modified equation for static contact conduction through solid contact area can be written as

$$Q_{i,j} = 4r_c(T_j - T_i)/(1/k_{pi} + 1/k_{pj}) \tag{14}$$

For implementation into DPS-CFD applications, the equation for collisional contact conduction through solid phase is modified as

$$Q_{i,j} = c' \frac{(T_j - T_i)\pi\, r_c^2 t_c^{-1/2}}{(\rho_{pi} c_{pi} k_{pi})^{-1/2} + (\rho_{pj} c_{pj} k_{pj})^{-1/2}} \tag{15}$$

More details of these equations can be found in the literature (Zhou et al., 2009; Zhou et al., 2010).

Coupling Scheme

The methods for numerical solution of DPS and CFD and their coupling schemes have been well established in the literature as reviewed by Zhu et al. (2007). The heat transfer model has been implemented into this approach by Zhou et al. (2009). The present work simply extends the approach to examine heat transfer mechanisms of gas fluidization with Geldart A powder.

SIMULATION CONDITION

The simulations are carried out in a container with a thickness of 4 particle diameters. For such geometry, three-dimensional DPS and two-dimensional CFD are used. The periodic boundary condition is applied to the front and rear direction. Table 1 lists the physical and geometrical parameters. The powder properties are based on a kind of silica-based fluid cracking catalyst. In the simulation, time step is a constant for solid and fluid, which is chosen to ensure the stability and accuracy of the numerical simulation according to particle properties and the expected maximum relative particle velocities (Schafer et al., 1996; Asmar et al., 2002). The total 10,000 particles are allowed to settle down under gravity without interaction with fluid. Then, the static bed is used as a base for the simulations where gas is uniformly introduced at the bottom.

Table 1: Physical and geometrical parameters used in the simulations.

Variables	Values	Units
Bed width×height	60×200	d_p
Cell size ($\Delta x \times \Delta z$)	2×2	d_p
Particle diameter, d_p	100	μm
Time step, Δt	1.38×10^{-6}	s
Particle density, ρ	1440	kg/m^3
Thermal conductivity of particles, k_p	0.84	W/(m·K)
Specific heat capacity of particles, c_p	840.0	J/(kg·K)
Initial temperature of particles and air	25	°C
Particle-particle/wall sliding friction, μ_s	0.3	-
Particle-particle/wall rolling friction, μ_r	0.01d_p	mm
Restitution coefficient	0.8	-
Particle Young's modulus, E	1×10^7	kg/(m·s^2)
Particle poisson ratio, ν	0.3	-
Hamaker constant, H_a	0 to 2.10×10^{-20}	J
Minimum separation, h_{min}	1	nm
Fluid density, ρ_f	By state equation*, $\rho = PM/(RT_f)$	kg/m^3
Fluid molecular viscosity, μ_f	By Sutherland's formula**	Pa·s
Fluid thermal conductivity, k_f	$2.87\times10^{-2} + 7.76\times10^{-5}\times(T_f+273)$	W/(m·K)
Fluid specific heat capacity, c_{pf}	$1002.74 + 1.23\times10^{-2}\times(T_f+273)$	J/(kg·K)

* P=101,325 Pa, M=0.029 kg/mol, R=8.314 J/(mol·K).
** $\mu_f = C_1 T^{3/2}/(T+C_2)$, where $C_1 = 1.511\times10^{-6}$ kg/(m·s·K$^{1/2}$), C_2 = 120 K.

RESULTS AND DISCUSSION

Overall Characteristics of Heat Transfer

A packed bed is agitated by the up-flowing interstitial gas, which is injected from the bed bottom. Bubbling fluidization begins when the gas superficial velocity (u_f) is above the minimum fluidization velocity (u_{mf}). The bed is heated by the introduced hot gas, and the averaged bed temperature with time is shown in Figure 2, where the dimensionless bed temperature T_b is defined as $(T_{bed}-T_0)/(T_{inlet}-T_0)$ (T_0 is the initial bed temperature, and T_{inlet} is the gas temperature at the inlet). It can be seen that the bed temperature increases faster with a higher u_f. Figure 3 shows the particle flow pattern and the heating process with T_{inlet} of 200 °C. It can be seen that, as shown in Figures 2 and 3, the temperature of individual particles is quite uniform and the bed temperature increases very

quick due to the rapid mixing and large particle-fluid contact area in bubbling gas fluidization.
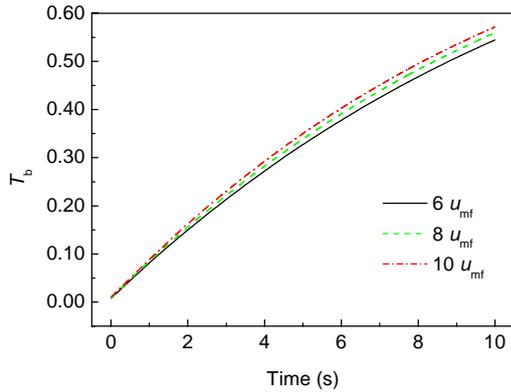
Figure 2: Bed temperatures in the heating up process under different u_f, where the u_{mf} is 0.72 cm/s and H_a is 4.20×10^{-21} J.
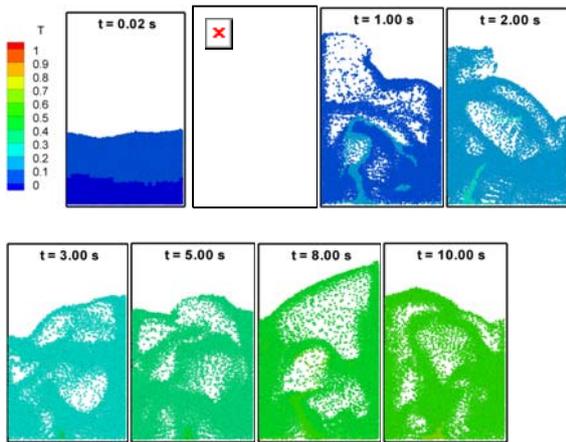
Figure 3: Heating up of a bubbling fluidized bed under the conditions of $H_a = 4.20 \times 10^{-21}$ J, $T_{inlet} = 200°C$, where u_f is 7.2 cm/s (the particles are colored by their dimensionless temperature, defined as $(T_i - T_0)/(T_{inlet} - T_0)$).

In the DPS-CFD simulation, the heat fluxes by particle-particle conduction and particle-fluid convection can be obtained quite readily. It should be noted that the heat heating the bed comes from the hot gas only in terms of particle-fluid convection mechanism, while the particle-particle conduction enhances the heat transfer process among particles and the uniformity of the bed temperature. In describing the heat transfer process, heat flux is related to the temperature gradient and reflects the real heat exchanged by different heat transfer mechanisms, and thus is used in this work. As an example, Figure 4 shows the variations of bed averaged heat fluxes of particles respectively by convection and conduction, and their relative contributions to the total heat flux by percentage. It can be seen that, as shown in Figure 4a, the averaged conductive and convective heat fluxes firstly increase and then decrease to nearly zero. At the first stage, because the bed is at low temperature and the temperature differences between particles and between particles and fluid are large, the heat fluxes that depend on the temperature gradient are hence large. With the heating of the bed, the temperature differences decrease and the

corresponding heat fluxes decrease. To examine the contributions of different heat fluxes, the percentages are obtained based on their absolute values at a particle scale, and shown in Figure 4b. It can be observed that the percentages of convective and conductive heat fluxes fluctuate around fixed values, and the particle-fluid convection is dominant. Figure 4c shows that the percentages of heat fluxes through different conductive mechanisms keep stable as well. The conduction through particle-fluid-particle is dominant in the present conditions.

(a)

(b)

(c)
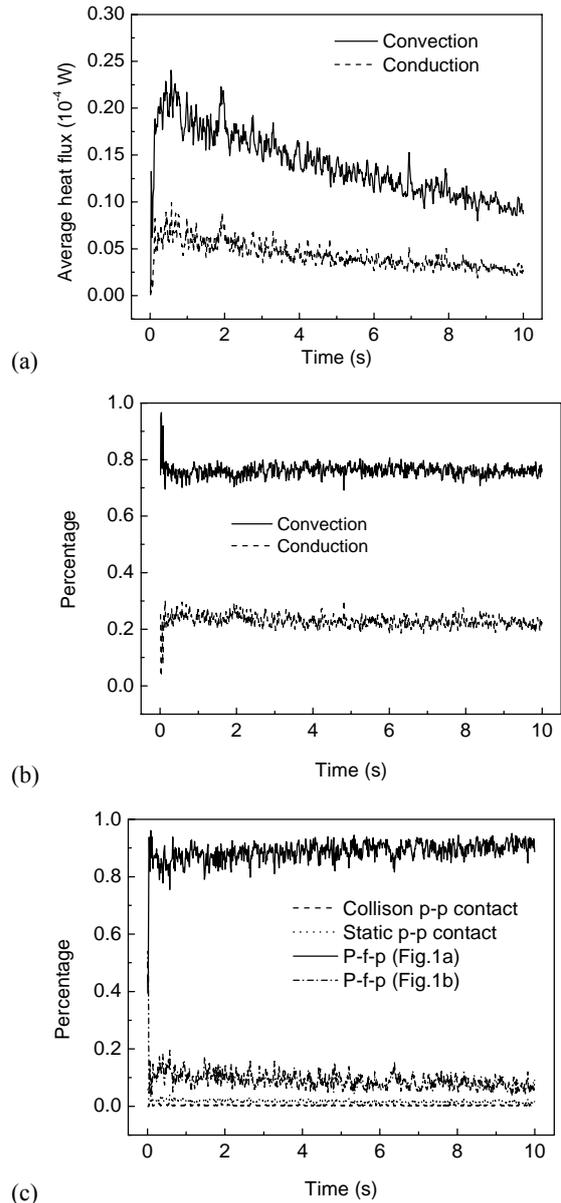
Figure 4: Heat fluxes of convection and conduction (a), their percentages to the total heat flux (b), and the percentages of different conductive mechanisms to conduction (c) under the condition of $H_a = 4.20 \times 10^{-21}$ J, $T_{inlet} = 200 °C$, $u_f/u_{mf} = 10$, and $u_f = 7.2$ cm/s.

Effects of Gas Superficial Velocity

The bubbling fluidization behaviour is determined by particle-particle and particle-fluid interactions. The effects of u_f have been examined by three cases at 6, 8 and 10 u_{mf}

4

in the present study. The variations of bed temperature have been shown in Figure 2. To investigate the heat transfer mechanisms, Figure 5 shows the variations of conductive and convective heat fluxes for the three cases. The heat fluxes are averaged values over the first 10 seconds. It can be seen that, with the increase of u_f, the convective heat flux increases while the conductive heat flux decreases. This is largely related to the changes of bed structures such as bed porosity or coordination number, as shown in Figure 6. The bed porosity increases with the increase of u_f, and then the corresponding fluid Reynolds number increases. Hence a high particle-fluid convective heat transfer coefficient.

The conductive heat transfer enhances the heat exchange between particles and is closely related to its surrounding particles. The averaged coordination number, the number of 'contacts' made by the neighbouring particles, of individual particles is obtained (Yang et al., 2000). Figure 6 shows that the average coordination number decreases with the increase of u_f. Less coordination number corresponds to the less particle-particle contact, and then the conductive heat transfer becomes weaker.
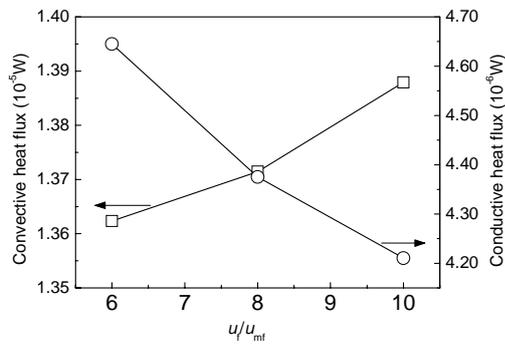
Figure 5: Convective (□) and conductive (○) heat fluxes as functions of u_f.
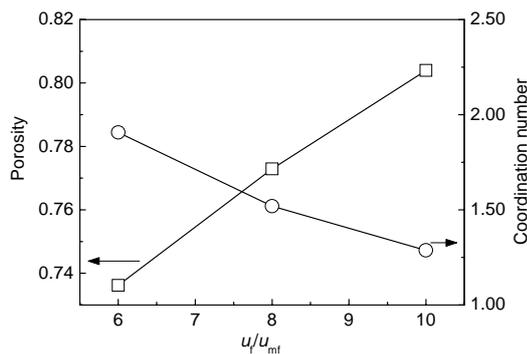
Figure 6: Bed averaged porosity (□) and coordination number (○) as functions of u_f.

Effects of Cohesive Force between Particles

The effect of van der Waals force on heat transfer is investigated with different H_a. Figure 7 shows that the bed temperature increases slower with a larger H_a. To investigate the heat transfer mechanisms, Figure 8 shows that the convective heat flux decreases and the conductive heat fluxes increases with the increase of cohesive force. Due to the dominance of convective heat transfer, the overall heat flux decrease, corresponding to the low bed

temperature. Figure 9 shows that the particle-fluid-particle non-contact heat flux decreases and the contact particle-fluid-particle heat flux increases with the increase of cohesive force.
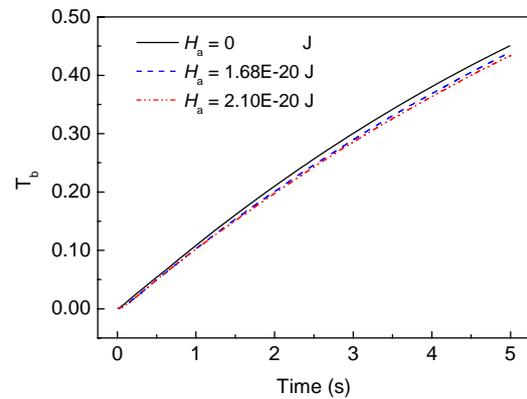
Figure 7: Bed temperature in the heating up process under different H_a, where the u_f is 7.2 cm/s.
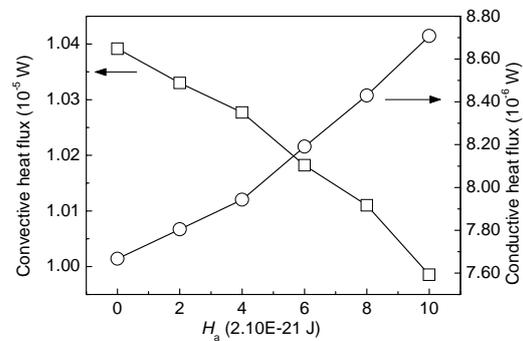
Figure 8: Convective (□) and conductive (○) heat fluxes as functions of H_a.
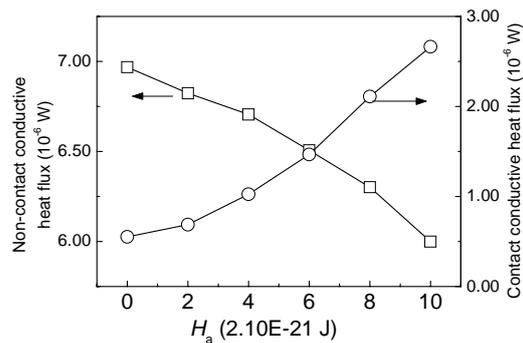
Figure 9: Heat fluxes of different conductive mechanisms through fluid as functions of H_a: non-contact (□) and contact (○).

Heat transfer process in bubbling fluidized bed is complicated and related to the contacts among particles and the bed structures. To investigate the mechanisms of the effects of van der Waals force, Figure 10 show the variations of bed averaged porosity and coordination number under different H_a. The bed averaged porosity decreases slightly with the increase of H_a. This trend partially explains the slower increase of the bed temperature with a larger H_a. Due to the increase of H_a,

5

the particles tend to form agglomerates and this is verified by the increased averaged coordination number as shown in Figure 10. It indicates that there are more particles in contact when the cohesive force is increased. Hence, the conduction is enhanced and the conductive heat flux increases.
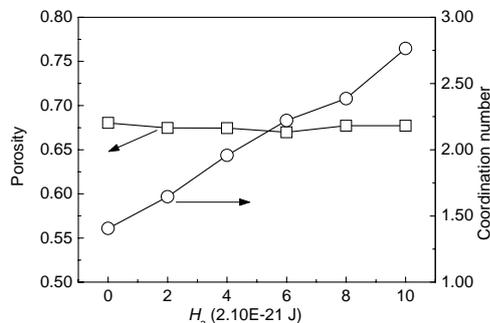
Figure 10: Bed averaged porosity (□) and coordination number (○) as functions of H_a.

CONCLUSION

The heat transfer behaviour of bubbling fluidized beds with a type A powder is studied by the coupled approach of DPS and CFD. The effects of gas superficial velocity and inter-particle van der Waals force are examined by the controlled parameters such as Hamaker constant. The results show that the convective heat flux increases with the increase of gas superficial velocity while the conductive heat flux decreases. With the increase of Hamaker constant, the convective heat flux decreases while the conductive heat flux increases. The heat flux by contact and non-contact conduction through the fluid composes the main part of the conduction in the present conditions.

ACKNOWLEDGEMENTS

REFERENCES

ASMAR, B.N., LANGSTON, P.A., MATCHETT, A.J. and WALTERS, J.K., (2002), "Validation tests on a distinct element model of vibrating cohesive particle systems". *Comput. Chem. Eng.*, 26, 785-802.

CHENG, G.J., YU, A.B. and ZULLI, P., (1999), "Evaluation of effective thermal conductivity from the structure of a packed bed". *Chem. Eng. Sci.*, 54, 4199-4209.

COLLIER, A.P., HAYHURST, A.N., RICHARDSON, J.L. and SCOTT, S.A., (2004), "The heat transfer coefficient between a particle and a bed (packed or fluidised) of much larger particles". *Chem. Eng. Sci.*, 59, 4613-4620.

CROWE, C.T., SOMMERFELD, M. and TSUJI, Y., 1998. Multiphase Flow with Droplets & Particles. CRC Press, Boca Raton Florida.

DI FELICE, R., (1994), "The voidage function for fluid-particle interaction systems". *Int. J. Multiphase Flow*, 20, 153-159.

DONG, K.J., YANG, R.Y., ZOU, R.P. and YU, A.B., (2006), "Role of interparticle forces in the formation of random loose packing". *Phys. Rev. Lett.*, 96, 145505.

GELDART, D., (1973), "Types of gas fluidization". *Powder Technol.*, 7, 285-292.

HAMAKER, H.C., (1937), "The London-van der Waals attraction between spherical particles". *Physica*, 4, 1058-1072.

ISRAELACHVILI, J.N., 1991. Intermolecular & Surface Forces. Academic, London.

JOHNSON, K.L., 1985. Contact Mechanics. Cambridge University Press, Cambridge.

KANEKO, Y., SHIOJIMA, T. and HORIO, M., (1999), "DEM simulation of fluidized beds for gas-phase olefin polymerization". *Chem. Eng. Sci.*, 54, 5809-5821.

KUNII, D. and LEVENSPIEL, O., 1991. Fluidization Engineering. Butterworth-Heinemann, Boston.

LAUNDER, B.E. and SPALDING, D.B., (1974), "The numerical computation of turbulent flows". *Comput. Methods Appl. Mech. Eng.*, 3, 269-289.

LI, J.T. and MASON, D.J., (2000), "A computational investigation of transient heat transfer in pneumatic transport of granular particles". *Powder Technol.*, 112, 273-282.

LI, J.T. and MASON, D.J., (2002), "Application of the discrete element modelling in air drying of particulate solids". *Drying Technology*, 20, 255-282.

MOLERUS, O. and WIRTH, K.E., 1997. Heat transfer in fluidized beds. Chapman and Hall, London.

SCHAFER, J., DIPPEL, S. and WOLF, D.E., (1996), "Force schemes in simulations of granular materials". *J. De Physique I*, 6, 5-20.

SCOTT, S.A., DAVIDSON, J.F., DENNIS, J.S. and HAYHURST, A.N., (2004), "Heat transfer to a single sphere immersed in beds of particles supplied by gas at rates above and below minimum fluidization". *Ind. Eng. Chem. Res.*, 43, 5632-5644.

WONG, Y.S. and SEVILLE, J.P.K., (2006), "Single-particle motion and heat transfer in fluidized beds". *AIChE J.*, 52, 4099-4109.

YANG, R.Y., ZOU, R.P. and YU, A.B., (2000), "Computer simulation of the packing of fine particles". *Phys. Rev. E*, 62, 3900-3908.

ZHOU, H.S., FLAMANT, G. and GAUTHIER, D., (2004), "DEM-LES simulation of coal combustion in a bubbling fluidized bed Part II: coal combustion at the particle level". *Chem. Eng. Sci.*, 59, 4205-4215.

ZHOU, H.S., FLAMANT, G., GAUTHIER, D. and FLITRIS, Y., (2003), "Simulation of coal combustion in a bubbling fluidized bed by distinct element method". *Chem. Eng. Res. Des.*, 81, 1144-1149.

ZHOU, Z.Y., YU, A.B. and ZULLI, P., (2009), "Particle scale study of heat transfer in packed and bubbling fluidized beds". *AIChE J.*, 55, 868-884.

ZHOU, Z.Y., YU, A.B. and ZULLI, P., (2010), "A new computational method for studying heat transfer in fluid bed reactors". *Powder Technol.*, 197, 102-110.

ZHU, H.P., ZHOU, Z.Y., YANG, R.Y. and YU, A.B., (2007), "Discrete particle simulation of particulate systems: Theoretical developments". *Chem. Eng. Sci.*, 62, 3378-3396.